REPORT:

A3.2.9: Guidelines for the measurement of key performance parameters of microfluidic connections including the identification of key properties in an interface

Deliverable 5 / Workpackage 3

www.mfmet.eu

This report was written as part of activity 3.2.9 from the EMPIR Establishing Metrology Standards in Microfluidic Devices (MFMET) project. The three-year European project commenced on 1st June 2021 and focused on providing a generic methodology of accurate measurement of a particular quantity in a microfluidic device by utilising standardised methods and reference documents, e.g. VIM & GUM. For more details about this project, please visit www.mfmet.eu

This report was written by:

Christina Pecnik	IMTAG	*cpecnik@imtag.ch*; *christina.pecnik.micro@outlook.com*
Henne van Heeren	EnablingMNT	*henne@enablingmnt.com*
Joris Kaal	CEA	*joris.kaal@cea.fr*
Elsa Batista	IPQ	*ebatista@ipq.pt*
Fernanda Saraiva	IPQ	*fsaraiva@ipq.pt*
Pedro Neves	IPQ	*peneves@ipq.pt*
Vania Silverio	INESC	*vsilverio@inesc-mn.pt*; *vania.silverio@tecnico.ulisboa.pt*
Huabing Yin	UofG	*Huabing.yin@glasgow.ac.uk*
Kevin Romieu	CETIAT	kevin.romieu@cetiat.fr
Florestan Ogheard	(former member)	
Nicolas Feltin	LNE	nicolas.feltin@lne.fr
Loïc Crouzier	(former member)	

The EMPIR initiative is co-funded by the European Union's Horizon 2020 research and innovation programme and the EMPIR Participating States

Contents

1. Scope

The objective of this document is to list the guidelines for the measurement of key performance parameters of microfluidic connections; this is based on the list of key properties of microfluidic interfaces. The motivation for this is that making microfluidic connections is often a laborious job and prone to reliability problems. This report is based on input from A3.1.1, A3.1.5, A3.2.1-A3.2.3, A3.2.5-A3.2.8, and available results from A3.2.4.

Activity number	**Activity description**	**Partners (lead in bold)**
A3.2.9 M20	Using input from A3.1.1, A3.1.5, A3.2.1-A3.2.3, A3.2.5-A3.2.8, and available results from A3.2.4, IMTAG with support from LNE, INESC MN, microfluidic, CEA, IPQ, CETIAT, CMI and UofG will produce guidelines for the measurement of key performance parameters of microfluidic connections including the identification of key properties in an interface. The guidelines will be submitted to the standardisation group such as ISO/TC48/WG3 and WG5, ISO/TC229, CEN/TC332/WG7. Once agreed by the consortium, the coordinator on behalf of IMTAG, LNE, INESC MN, microfluidic, CEA, IPQ, CETIAT, CMI and UofG will submit the guidelines to EURAMET as D5: 'Guidelines for the measurement of key performance parameters of microfluidic connections including the identification of key properties in an interface'.	**IMTAG**, LNE, INESC MN, UofG, microfluidic, CEA, IPQ, CETIAT, CMI

2. Materials in microfluidics

There are many different materials in use in microfluidics. The reliability of microfluidic devices is defined by the interplay of all materials involved. The choice of materials depends mostly on the specific use and function of the microfluidic device, but also the availability of fabrication technology and productions cost can play an important role in it. In general, the three most commonly used material groups in microfluidics can be defined:

- Polymers
- Inorganic materials (glass, silicon, oxides)
- Metals

For the polymers, three main classes can be defined as: thermosets, thermoplastics and elastomers. Particularly thermoplastic polymers are used as base materials, such as COC (cycloolefin copolymer) or COP (copolyester thermoplastic elastomer), since they have a good resistance to creep and are electrically isolated. In addition, they are the most suitable for high volume production techniques such as injection moulding. Furthermore, they have a low autofluorescence, are biocompatible and exhibit a low water absorption. Thermoplastics can also be found in fluidic connectors, where they are most often combined with elastomers such as silicone or FFKM (perfluoroelastomer).

The most often used glass types for microfluidic components are D236® T eco, D236® bio and MEMpax®. In general, all three glass types are suitable for microfluidic applications, but their use may differ depending on specific requirements. D236® bio exhibits a very low intrinsic autofluorescence across the UV to NIR spectrum compared to D236® T eco. Furthermore, spectral transmittance provides information about the optical properties of the substrate, such as optical density, reflectance, or transparency. If glass is combined with silicon, MEMpax® should be chosen to avoid stresses due to thermal expansion. Such induced stresses can, in the worst case, lead to fracture of the entire component.

There is a strong preference in the industry for COC/COP, glass, glass/Si and PMMA (polymethylmethacrylat). Glass is especially used in demanding applications, particularly for devices that are reused frequently and for long periods of time and/or operates at higher pressures and temperatures. However, glass is sometimes used in single-use applications, for instance Point-of-Care applications, or high density multiplexing such as next generation sequencing. COC/COP is mainly used for disposables for Point-of-Care testing. PC (polycarbonate) and PS (polystyrene) are popular choices for those that are using cell cultures or organ-on-chip for experiments and tests. Often combinations of materials are used.

In summary, the material used depends on its function in the microfluidic device: base material, fluidic channel or electrode. Although there is a wide range of materials used, for the purpose of this report

we will focus on the wetted materials, i.e. the materials that are in contact with the fluids, the top five being:

- **COC/COP** for base material and fluidic connectivity,
- **glass** for base material,
- **PEEK (polyetheretherketone)** and **PFTE (polytetrafluoroethylene)** for fluidic connectivity and
- **PC** for fluidic connectivity.

Less often used are:

- PMMA for base material,
- PP (polypropylene), PS, silicone, FFKM for fluidic connectivity,
- Pt and Au for electrical connectivity,
- stainless steel for fluidic connectivity and
- fused silica for fluidic connectivity.

3. Dimensions and connectors in microfluidics

Microfluidic structures are produced on flat substrates or chips (except in the case of 3D manufacturing). The manufacturing of microfluidics is mainly based on:

1) Injection molding (polymers).
2) Etching of glass.
3) Hot embossing (polymers).

Each of these technologies has its own merits and result in products with specific characteristics:

Table 1: Technical aspects of the different microfluidic fabrication technologies.

Geometric feature	**Glass: planar processing**	**Polymer: injection molding**	**Polymer: embossing**
typical chip sizes [mm]	15 x 15; 15 x 22.5; 15 x 30; 15 x 45	credit card format or microscope slide (25 x 75)	credit card format or microscope slide (25 x 75)
chip thickness [mm]	thinnest: 0.03 standard: 0.7, 1.1, 2.0	standard: 0.6 thickest: 5 (preferably <1.5)	
channel width [µm]	Mask width + 2* channel depth; min. mask width at 10, 1 on special request	> 50	
etch depth [µm]	0.01 - 500	< 70	
min. spacing between structures [µm]	5 +2.6*etch depth	Same as structure height, but at least 50	
aspect ratio for the channels	< 1:2	< 1:2	
electrodes [µm]	min. width = 2 standard width = 5 thickness = 0.05 - 1		

(these values are an indication only, exact specifications can vary between suppliers.)

These technologies are described in the White Paper “Design for Microfluidic Device Manufacture Guidelines” [1].

Although several chip sizes are used for microfluidics, substantial numbers of commercial microfluidic devices have the exact outer dimensions of standard microscope slides or microtiter plates. As glass based microfluidic chips are often much smaller the pro-forma standards for glass chip dimensions

are based on multiples of 15 mm. Apart from gluing connectors on a chip, glass chips often use clamping systems to connect to tubing. In contrast, moulded plastic devices often use mini-Luers. This section introduces commonly used connectors, their size and location on commercial devices.

An overview of the most used microfluidic connectors is given below (Figure 1):

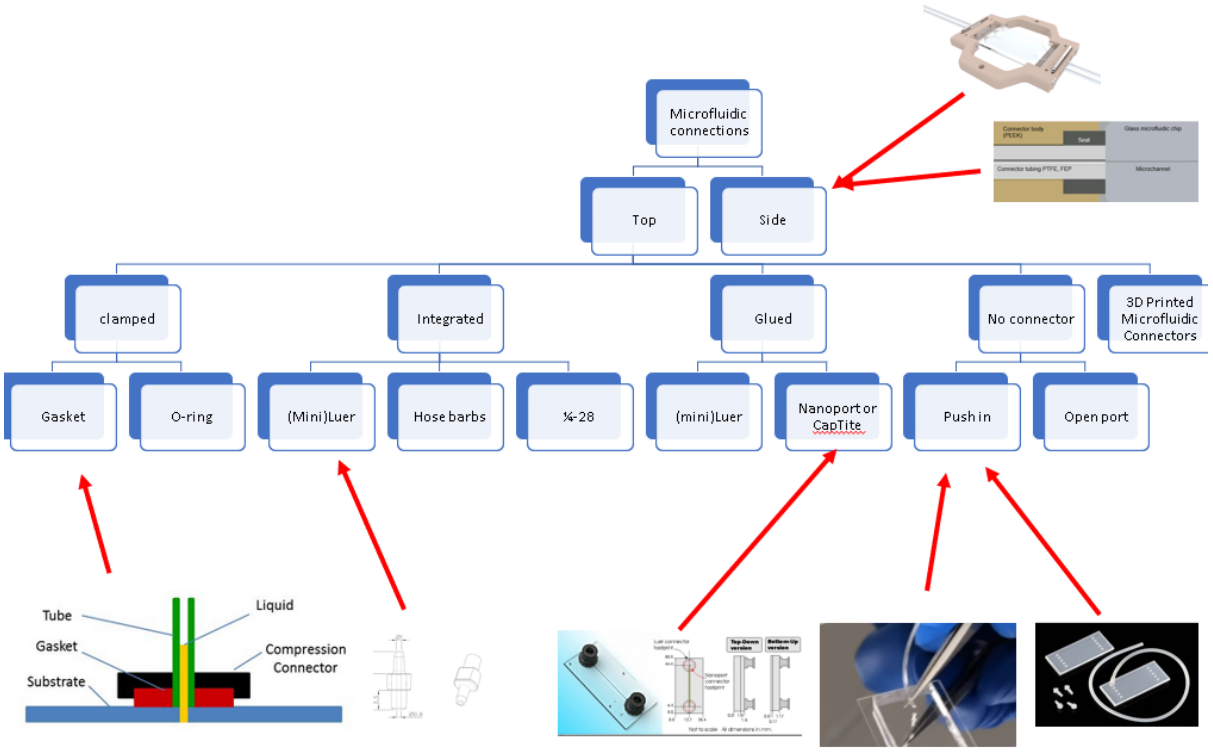

Figure 1: Overview of microfluidic connectors to chips or substrates.

4. Key performance parameters

The choice of materials and connections for microfluidic devices play a crucial role in their efficient and reliable operation. The performance of these two aspects directly affects the overall functionality and reliability of the device. Therefore, it is crucial to measure and evaluate specific parameters of these aspects to optimize performance.

The following key parameters have been identified, with the help of end-users from industry, for **connectivity** between fluidic passages of microfluidic components and devices:

- **Dead volume**, i.e. the portion of the internal volume of a system that is not part of a continuous flow-path (definition from ISO/FDIS 10991 [2]). Dead volume is always undesirable in any fluidic application as it can contribute to diffusion effects and adsorptive loss due to the increased surface area. However, in microfluidics, dead volume poses an even more detrimental threat as it creates regions where air bubbles or compressible gas can trap. These air pockets can lead to bubble release, as well as flow pulsing due to the presence of compressible gas in the flow path. Furthermore, when working with live cells, if the cells are exposed to air, cell death will result. Therefore, special care needs to be taken to eliminate dead volume in microfluidic systems.
- **Footprint**, i.e. the space that a connector takes up in the microfluidic device. For example, when designing a ISO 22916:2022 compatible 15x15 mm building block, or a microscope-slide-sized chip, and one has the choice between integrating mini-Luers or regular ones, their footprint can be the decisive factor.
- **Ease of operation**, including:
  - the time needed for mounting the connector, and for connecting/disconnecting it
  - the tooling required for mounting the connector, and for connecting/disconnecting it
- **Pressure drop**, i.e. difference of pressure between two positions in the flow path (definition from ISO/FDIS 10991 [2]).
- **Leakage rate**, i.e. the flow rate or flow rate range coming out of the fluidic path through the connector parts for a given pressure or pressure range respectively.
- **Burst pressure**, i.e. the pressure at which the sealing function, the continuity of the fluidic path and the integrity of the connector's assembly is not ensured.
- The **residence time distribution** is the probability distribution of the time a piece of material is likely to spend in the process. A characteristic to describe it is the solution exchange time. The most straightforward way to determine the residence time distribution is to measure the system response for a short tracer pulse. Some dead volumes can introduce mixing, which slows down, how fast one solution can be switched to another through interfacing ("chemical low-pass filter"). Another characteristic is a "mechanical low-pass filter" describing how much the rapid pressure

change would be damped (e.g. if inside the controller the pressure would rise abruptly, how quickly would the pressure and flowrate change in the chip).

Furthermore, task A1.1.2 described the **dead volume** as a kind of “buffer volume”. Consequently, microfluidic designers and manufacturers of microfluidic devices try to minimise the dead volumes in their fluidic products. In general, the dead volume can only be tested on existing microfluidic devices. Such exemplary devices, like the golden standards made of glass and polymer with their corresponding connections, will be produced, assembled, and subsequently tested. Simultaneously, the **ease of operation** will be tested as well on the golden standards and documented at a later stage. It would also be interesting to test whether or not connections can be undone in a non-destructive manner. For example, if one wants to be able to re-use cards with building blocks attached to them, one needs to be able to disconnect them. This aspect especially comes into play when using protocols that require virgin chips, or protocols that cannot be repeated infinitely and require frequent chip-refreshment. Also from a recyclability point-of-view, this is an issue that needs to be addressed.

Leakage rate and **burst pressure** have been extensively defined and discussed in task A1.2.4. Additionally, deliverable D1 presents guidelines and a test protocol for leakage and burst pressure of microfluidic devices.

The **pressure drop** is a critical performance parameter for microfluidic connections, as it directly impacts the flow rate and efficiency of the fluidic system. Pressure drop refers to the difference in pressure across the connection due to fluid flow, and it can be influenced by various factors such as the size and shape of the connection, the fluid properties, and the flow rate. Particularly, the **wettability** and the **roughness** of surfaces can strongly influence the fluidic behaviour. Wettability refers to the ability of a surface to attract or repel a liquid and can be characterized by the contact angle between the liquid and the surface. In microfluidic connections, surfaces with high wettability tend to reduce pressure drop by promoting laminar flow and minimizing fluid adhesion to the surface. Conversely, surfaces with low wettability tend to promote turbulent flow, leading to higher pressure drop due to increased fluid resistance. Surface roughness, on the other hand, refers to the irregularities and deviations on the surface of the microfluidic connection. Higher surface roughness can lead to increased pressure drop due to increased friction between the fluid and the surface. In contrast, smoother surfaces tend to reduce frictional losses and promote laminar flow, leading to lower pressure drop.

Choosing **materials** with high wettability and low surface roughness can lead to reduced pressure drop and improved performance of microfluidic devices. Accurately measuring and evaluating these properties is essential for optimizing the performance of microfluidic devices, as it can help identify connections with high resistance and improve the overall efficiency of the system.

To characterize and validate the fluid velocity profiles within microchannels, one can measure the pressure drop data by **Particle Image Velocity (PIV)** technique. This knowledge aids in optimizing device performance, identifying potential flow issues, and advancing various microfluidic applications, such as lab-on-a-chip devices, biomedical diagnostics, and microreactors.

In the following, test methods, that can be used to measure the wettability and the surface roughness, will be discussed, and the test protocols required for such measurements will be provided. Further information will be provided in future guidelines on how to evaluate such data and optimize connections for improved performance. Furthermore, we briefly explain the micro Particle Image Velocity (µPIV) technique, its working principles and how can it be applied to micro flow.

4.1. Wettability on microfluidic surfaces

This section uses the definitions of wettability established in activities A3.2.2, using the standards ISO 19403-1 [3] and ISO 19403-2 [4]. Furthermore, the described method focuses on the evaluation of wettability on flat surfaces ("open" microfluidic substrates) and not in channels ("closed" microfluidics with fully circular cross-sectional channels). There are various approaches in research and publications ([5], [6], [7], [8], [9], [10]), but up to this date there is no uniform and unambiguous method for measuring the contact angle in a channel. Measurement setup and devices for such purposes are also not defined in a uniform way or even to be purchased.

The documented example of this test protocol was performed in the liquid flow laboratory at CETIAT (Villeurbanne, France) and describes in detail the measurand (contact angle) and the property assessed (wettability) quantified by the surface energy of a given material.

The materials used in the documented example were glass slides (D263® bio) with a thickness of 1 mm, a width of 25 mm and a length of 75 mm, provided in a sealed box by IMTAG (Greifensee, Switzerland).

4.1.1. Measurement setup

Figure 2 shows the measurement setup used to measure the contact angle on the specimen. The **test conditions** to measure the contact angle on flat surfaces are described below:

a) Setting up the contact angle measuring system should be free of vibrations, intense air flow, and intense exposure to light from the outside. The system should be aligned horizontally.
b) Test conditions should be carried out at (23 ± 2)°C and a relative humidity at (50 ± 5)%; the test media should have the same temperature.
c) The sample specimen should be placed on a sample holder, its height should be positioned in the lower half of the image and horizontally aligned.
d) The chosen test liquid should be prepared and filled in a syringe without contamination or bubbles.
e) The needle/cannula is moved in the upper margin of the image; focus, contrast and brightness should be adjusted. The magnification should be adjusted to have the width of the contour of the drop to take up 2/3 of the measurement image.

Shape standard samples CP24 have been used to calibrate the Young-Laplace method for measuring the contact angle. These standard samples allow the contact angle measurement to be calibrated with an accuracy of 0.1°. A detailed procedure of the calibration steps is described in the report of activity A3.2.5, in which the manual measurement of the contact angle gave the best accuracy compared to automatic or semi-automatic plugins.

For this documented example, the **OWRK model** was used (also described in the report of activities A3.2.2 and A3.2.5) to assess the surface energy of a D263®bio specimen three liquids, water, di-iodomethane and ethylene glycol, of known surface tension, dispersive fraction, and polar fraction, which are described in the ISO 19403-2 standard [4] were used. Three contact angle measurements were conducted per type of liquid.

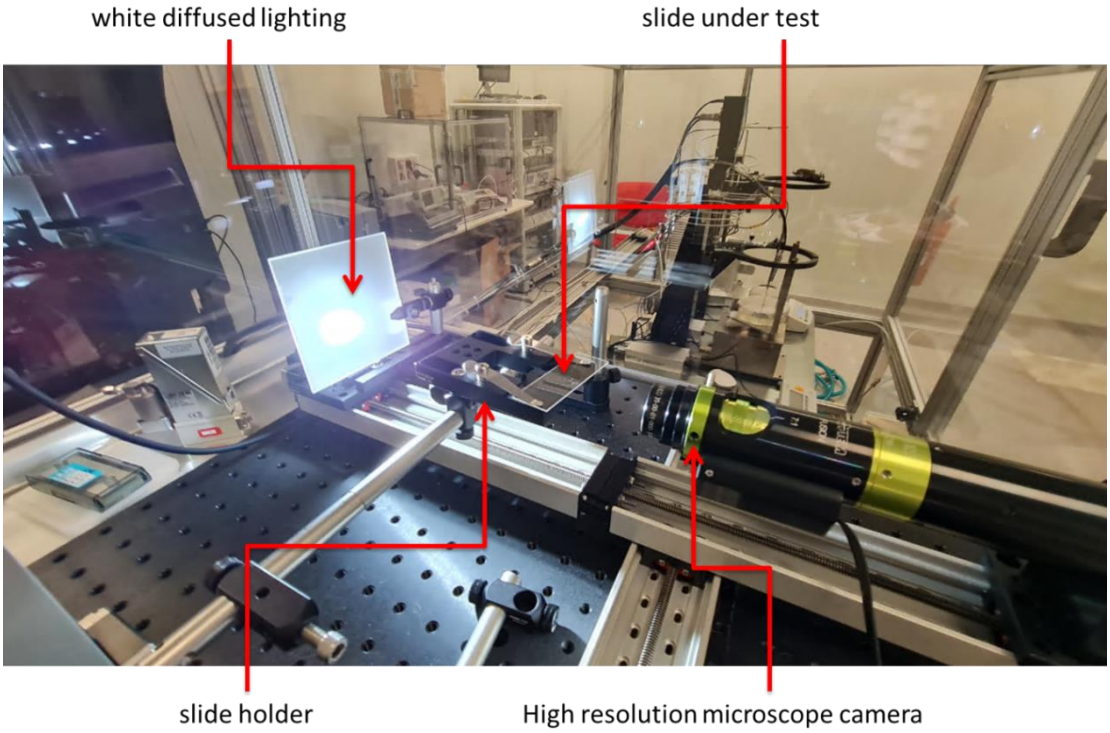

Figure 2: Measurement setup for contact angle measurements on flat surfaces.

4.1.2. Results

Fehler! Verweisquelle konnte nicht gefunden werden. presents the results of the contact angle measurements.

Table 2: Contact angle measurements on D263® bio specimens.

Test liquid	Water	Di-iodomethane	Ethylene glycol
Contact angles θ [°]	26.57	38.04	41.19
	21.56	34.02	33.22
	20.66	41.09	34.89
Average $\bar{\theta}$ [°]	22.93	37.71	36.43
Estimation of standard deviation $\widehat{S_{\bar{\theta}}}$ [°]	3.18	3.55	4.20

Fehler! Verweisquelle konnte nicht gefunden werden. and **Fehler! Verweisquelle konnte nicht gefunden werden.** show the relevant parameters for the OWRK model and the corresponding plot, respectively.

Table 3: Calculations for the OWRK model and its experimental plot.

Test liquid	$\bar{\theta}$	$\cos(\bar{\theta})$	σ_l^D	σ_l^p	σ_l	x	y	$U_{k=2}(y)$
	°						(mN/m)$^{1/2}$	(mN/m)$^{1/2}$
Water	22.93	0.92	21.8	51.0	72.8	1.53	14.98	0.34
Di-iodomethane	37.71	0.79	50.8	0.0	50.8	0.00	6.38	0.27
Ethylene glycol	34.89	0.82	30.9	16.8	47.7	0.74	7.81	0.37
Source	Measured by CETIAT		Data from ISO 19403-2:2017			See OWRK model below		

- Where, according to the OWRK model: $x = \frac{\sqrt{\sigma_l^p}}{\sqrt{\sigma_l^D}}$
- $y = \frac{\sigma_l(\cos\theta+1)}{2\sqrt{\sigma_l^D}}$
- $U_{k=2}(y)$ is the expanded uncertainty of y for $k = 2$, calculated at $\theta = \bar{\theta}$:

$$U_{k=2}(y) = 2\,u_c(y) = 2\left|\frac{\mathrm{d}y}{\mathrm{d}\theta}(\bar{\theta}).\mathrm{d}\bar{\theta}\right| = 2\,\frac{\sigma_l \sin\bar{\theta}}{2\sqrt{\sigma_l^D}}\widehat{S_{\bar{\theta}}}$$

A Monte-Carlo estimation of the uncertainty gives the same values.

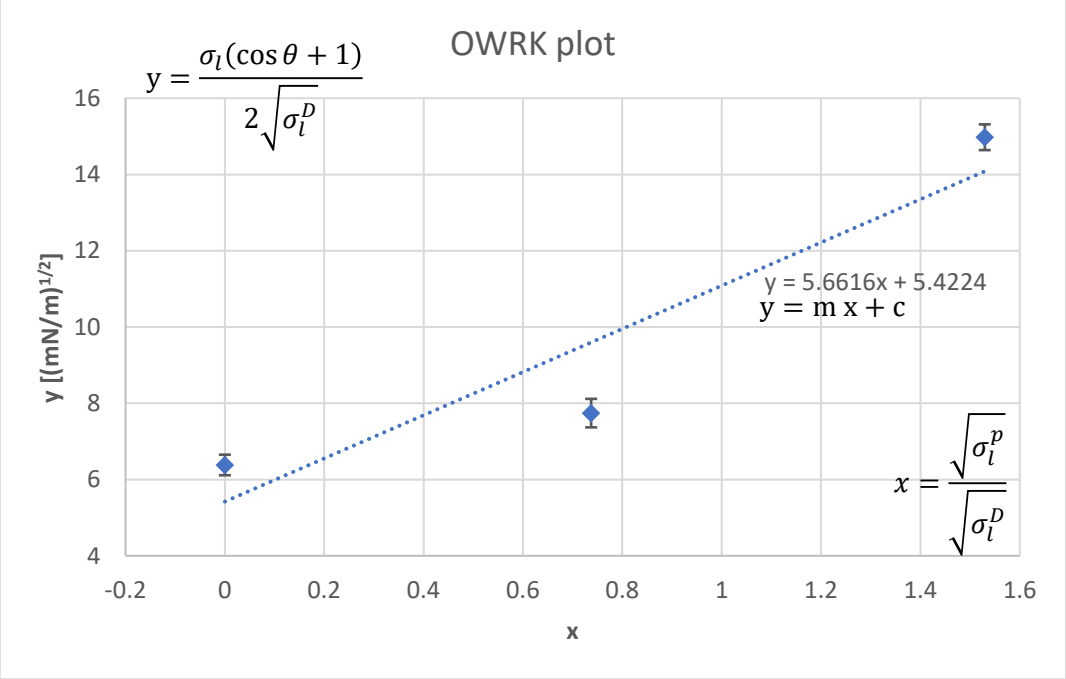

Figure 3: Experimental OWRK plot for a D263® bio specimen.

A linear regression on the plot above allows obtaining:

- the squared root of the polar fraction $m = \sqrt{\sigma_s^p}$ as the slope of the linear fit

- the squared root of the dispersive fraction $c = \sqrt{\sigma_s^D}$ as the y-intercept of the linear fit

The numerical values obtained are in **Fehler! Verweisquelle konnte nicht gefunden werden.**:

Table 4: Polar and dispersive fractions from the OWRK plot, deriving the polar and dispersive components of the surface energy according to the Fowkes theory.

Polar fraction		**Dispersive fraction**	
m [(mN/m)^{½}]	5.66	c (mN/m)^{½}]	5.45
$m^2 = \sigma_s^p$ [mN/m]	32.04	$c^2 = \sigma_s^D$ [mN/m]	29.65

Finally, the surface energy σ_s can be calculated as the sum of the polar and dispersive component, which results in the surface energy σ_s:

$$\sigma_s = \sigma_s^D + \sigma_s^p = 32.04 + 29.65 = 61.69\ \mathrm{mN/m}$$

for the tested D263® bio specimen.

To evaluate the uncertainty on this result, the square root of the maximum of the fit residuals has been calculated. As an example, the absolute value of the square root difference between the y-intercept and the value obtained for di-iodomethane results in $\sqrt{6.38 - 5.66} = 0.97$.

The final value of the uncertainty is rounded to 1 mN/m at *k*=1 (68 % confidence interval).

Therefore, the surface energy σ_s of D263® bio can be expressed as 61.69 mN/m with an uncertainty of 2 mN/m (*k*=2, 95 % confidence interval).

4.2. Surface roughness measurements

For the following section, the definitions for the various surface roughness parameters, **S_a and/or R_a**, are provided in the report of activity A3.2.4. Depending on the measurement method for surface roughness, there are various standards that can be applied, their test conditions and evaluation. Three methods were chosen to measure and evaluate the surface of selected specimens:

- Confocal microscopy ([11], [12]; older evaluation versions according to [13])
- Atomic force microscopy ([11] and [12])
- Stylus profilometry ([14], [15], [16], [17])

Table 5 displays the metrological limits with the measurement of surface texture. The main parameters to consider when choosing a suitable method for surface roughness measurement are the range and resolution of the instruments. For the stylus profilometry, it can vary widely depending on the specific instrument and measurement conditions. However, as a general guideline, the measurement range of a typical stylus profilometer is in the range of several µm to several mm, while the resolution is typically in the range of nm to µm [17].

Table 5: Metrological limits associated with the measurement of surface texture by AFM and confocal microscopy.

Method	Lateral resolution	Vertical resolution	Lateral range	Vertical range
Atomic Force Microscopy	Tip radius < 10nm	< 1 nm	Several tens of µm*	5 – 10 µm
Confocal Microscopy	~ 0.2 µm [7-10]	~ 0.5 µm [7-10]	Field of view: Few 10µm up to few 1000µm xy stage: up to 10mm - 100mm	<1mm up to several mm
Stylus profilometer	Tip radius = 2 µm	2 nm	---	Up to 500 µm (± 250 µm)

* Curvature effects may occur for large displacements on some instruments

The specific test conditions and detailed test protocols for each of these three methods were established in the report of activity A3.2.4. For each method one documented example was performed at one partner: confocal microscopy at IMTAG (Greifensee, Switzerland), atomic force microscopy at LNE (Paris, France) and stylus profilometry at IPQ (Caparica, Portugal).

The materials used for all documented examples taken from existing, unbonded flow cells made of glass, provided by IMTAG (Greifensee, Switzerland). The glass type is D263®bio and the substrate contains 100µm deep wet etched channels. In order to make the flow cell design unrecognisable, the samples were cut into slides by laser dicing (see Figure 4).

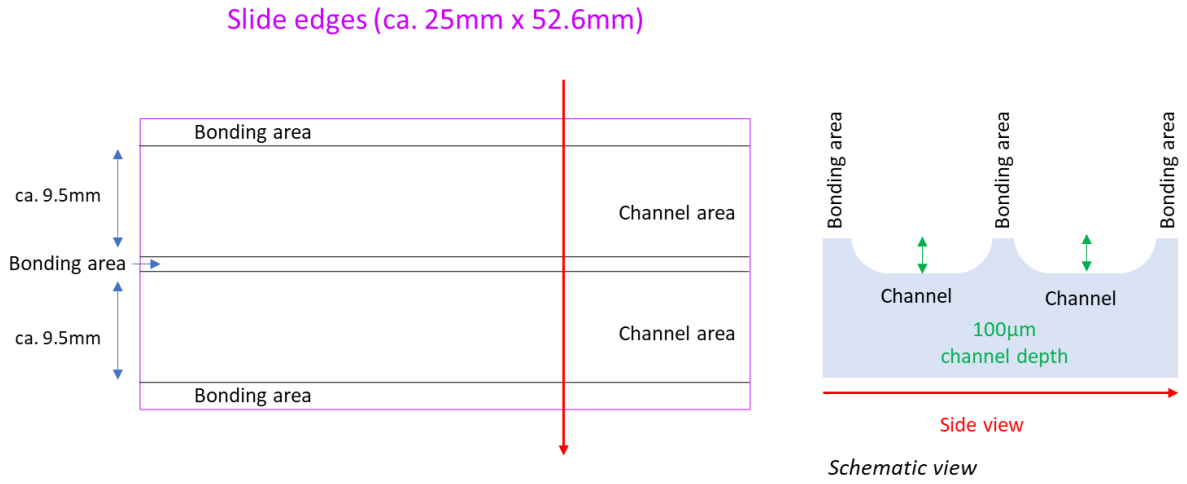

Figure 4: Slides provided for surface roughness measurements (view from the top on the left, sideview on the right).

The slides contain both parts of areas interesting for surface roughness measurements: the **bonding area** and **channel area**. Both areas aimed at having a low roughness value: bonding can only be achieved with values below 1 nm and the flow of fluids through the channels is considered to be best on smooth surfaces. Due to its wet etch process it is assumed that the channel area might be slightly rougher than the bonding area.

4.2.1. Confocal microscopy

The test protocol and the measurement setup are described in the report of A3.2.7. The results of the measurements, using a VK-9700 microscope, in the bonding and channel area are presented below:

Table 6: Results of the surface roughness analysis according to JIS B0601: 2001 (ISO 4287: 1997 [13]). Three measurements per area were conducted.

Roughness measurement	**Bonding area [µm]**			**Channel area [µm]**		
& value	**1**	**2**	**3**	**1**	**2**	**3**
Line roughness R_a	0.008	0.009	0.009	0.007	0.007	0.006
Surface roughness R_a	0.012	0.007	0.014	0.008	0.006	0.007

Confocal microscopy can be a suitable instrument for measuring surface roughness, including for glass etched channels. However, it is important to consider the resolution limit of the microscope and whether it is appropriate for the scale of the surface features being measured. This has already been mentioned in previously in Table 5 (lateral resolution: ~ 0.2 µm; vertical resolution: ~ 0.5 µm).

The roughness values of the blank substrate before processing are specified (and confirmed by the supplier) to be below 0.5nm. The measured roughness values after processing are still extremely small (between 6 nm and 14 nm), which is very well below the resolution limit of many confocal laser microscopes.

The resolution limit of a microscope is determined by the diffraction limit, which is dependent on the wavelength of the light used and the numerical aperture of the objective lens. In general, the resolution limit of a confocal microscope is around half the wavelength of the laser light used (typically in the range of (400-700) nm for visible light), which means that the VK-9000 microscope may not be able to accurately resolve features that are smaller than a few nm.

For the sake of completeness, measurements were carried out and evaluated. The measured values cannot be regarded as meaningful and do not allow any significant conclusions to be drawn about the actual surface roughness. Therefore, it is important to consider the resolution limit of your confocal laser microscope and ensure that it is appropriate for the scale of the surface features you are trying to measure. If the microscope cannot resolve the surface features with sufficient accuracy, other instruments or techniques may need to be considered, such as atomic force microscopy.

4.2.2. Atomic force microscopy

The test protocol and the measurement setup are described in the report of activity. A3.2.7. In the following, the results of the measurements, using a Veeco Dimension 3100 AFM, in the bonding and channel area are presented below:

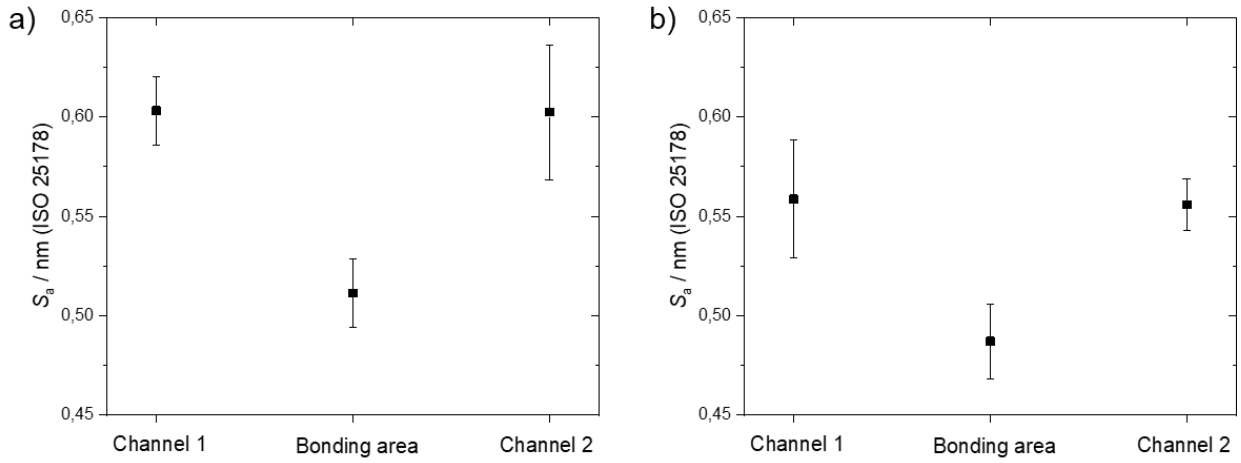

Figure 5 : Results of the roughness measurements for the two specimens a) Sample 1 and b) Sample 2. The results show the average of the three measurements for S_a for each area. The error bars represent the standard deviation (SD) between the three measurements for each area.

Table 7: Results of the roughness parameter S_a for the three specimens Sample 1-3. The results after ± express the standard deviation (SD) between the three measurements for each area (k = 1).

	S_a (channel 1) ± SD [nm]	S_a (bonding area) ± SD [nm]	S_a (channel 2) ± SD [nm]
Sample 1	0.60 ± 0.02	0.51 ± 0.02	0.60 ± 0.03
Sample 2	0.56 ± 0.03	0.49 ± 0.02	0.56 ± 0.01
Sample 3	NA*	0.46 ± 0.01	NA*

* not applicable

For each specimen, the measured roughness in the bonding area is slightly lower than in the channels. Furthermore, for each specimen, the measured roughness is equivalent for both channels (1 and 2). A slight shift is observed between the two specimens, both for the measurements in the channels and those on the bonding area. This effect could be attributed to wear (different radius of curvature) of the AFM tip.

4.2.3. Stylus profilometry

The test protocol and the measurement setup are described in the report of A3.2.7. The results of roughness parameters obtained by a Mahr reference measuring station MarSurf GD 140, which includes a stylus instrument with a probe arm length of 45 mm, *Ra*, *Rz*, *Rt*, *Rq*, *Rv*, *Rp, Rsk* and *Rsk* for 3 different slides in the bonding and channel area are presented below:

Table 8: Results of the roughness measurements parameters using the stylus instrument.

Slide		***Ra*** **/nm**	***Rq*** **/nm**	***Rz*** **/nm**	***Rt*** **/nm**	***Rp*** **/nm**	***Rv*** **/nm**	***Rsk*** **/nm**	***Rku*** **/µm**
I	channel 1	1.4	1.7	8.2	11.5	4.2	4.0	-83.9	3.571
	channel 2	1.3	1.6	7.8	9.9	3.6	4.0	-381.3	3.278
	Average I	1.3	1.7	7.9	10.7	3.9	4.0	-232.6	3.425
II	channel 1	1.3	1.6	7.8	10.7	3.9	3.9	-74.6	3.530
	channel 2	1.3	1.7	8.4	11.6	4.1	4.3	-238.4	3.485
	Average II	1.3	1.7	8.1	11.1	4.0	4.1	-156.5	3.507
III	channel 1	1.4	1.8	8.2	12.8	4.2	4.0	142.2	4.676
	channel 2	1.5	1.9	8.6	13.2	4.4	4.2	365.0	5.072
	Average III	1.4	1.9	8.4	13.0	4.3	4.1	253.1	4.874
Result value (Average)		**1.3**	**1.7**	**8.1**	**11.6**	**4.1**	**4.1**	**-45.2**	**3.935**
standard deviation		0.1	0.1	0.2	1.2	0.2	0.0	261.5	0.814

	Ra **/nm**	***Rq*** **/nm**	***Rz*** **/nm**	***Rt*** **/nm**	***Rp*** **/nm**	***Rv*** **/nm**	***Rsk*** **/nm**	***Rku*** **/µm**
Bonding area	**1.4**	**1.8**	**8.4**	**11.3**	**4.0**	**4.4**	**-383.0**	**3.262**
standard deviation	0.2	0.3	1.0	1.4	0.4	0.6	195.7	0.304

No significative variations were found between the results of the roughness parameters measured, *Ra*, *Rz*, *Rt, Rq*, *Rv* and *Rp*, neither inside the channels nor in the bonding areas in all slides analysed. This means that the manufacture process used to generate the etched channels shows no deterioration of the bonding area and a minor deterioration on the channel surface for the parameters studied. The difference found for the *Rt* parameter can be explained by a possible random peak or valley scanned in one of the measured line profiles.

Skewness parameter (*Rsk*) is a measure of the asymmetry of an amplitude density curve. Negative skewness indicates a surface with good bearing properties.

Kurtosis parameter (*Rku*) is a measure of the slope of an amplitude density curve. For profile values with normal distribution, *Rku* = 3.

4.3. Basic principles of particle image velocimetry

To measure flow-related characteristics Particle Image Velocimetry is a commonly used method. Particle Image Velocimetry (PIV) consists of recording the displacement of neutrally buoyant microparticles in a fluid flow. The particles are selected to have a density similar to that of the fluid, such that the particles follow (trace) the flow faithfully without influencing the flow itself [18]. Images of the flow with its particles are taken at well-defined time intervals. Next, they are analysed using a certain correlation method of choice and the particles' displacement vectors are obtained as displayed schematically in Figure 6. The images are divided into small regions known as interrogation areas, which contain small groups of particles. The statistical analysis of these interrogation windows between consecutive images gives the velocity of the particles and thus the local velocity of the flow.

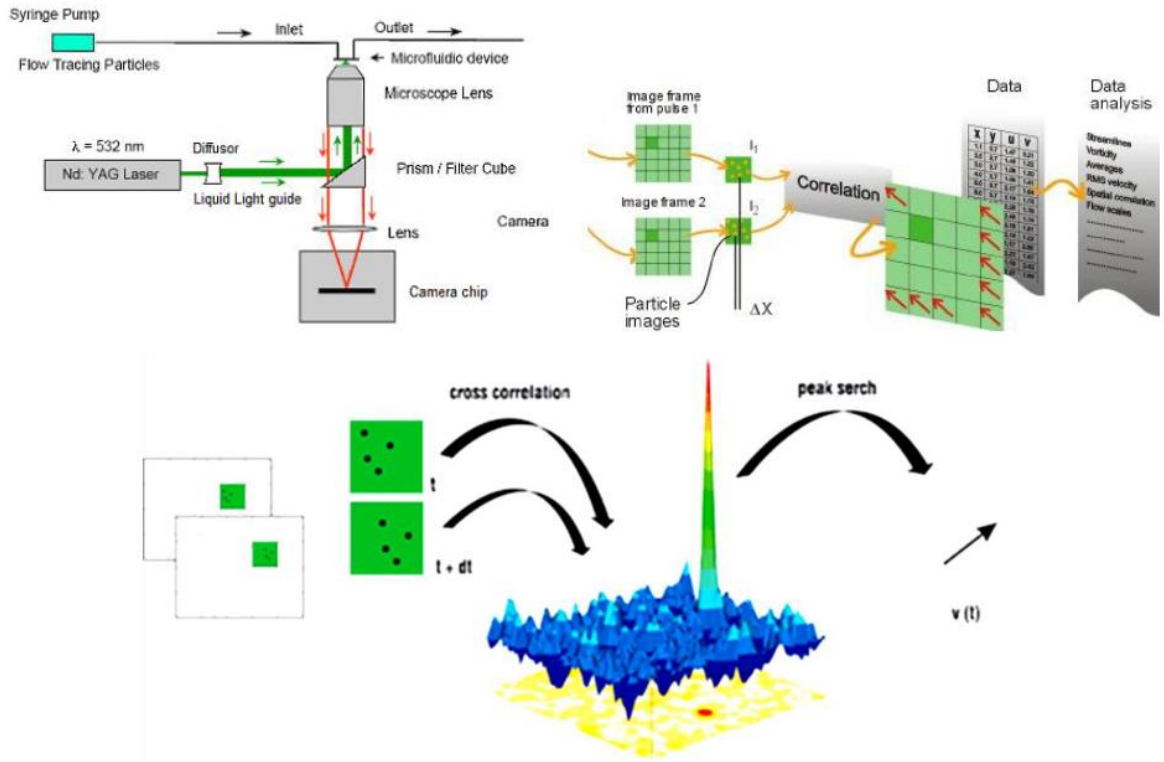

Figure 6: Micron-Resolution Particle Image Velocimetry (µPIV) schematics [19].

4.3.1. Light sheet vs. volume illumination

In normal PIV, a laser light sheet illuminates and defines the measurement plane, captured by a camera positioned perpendicularly to the light sheet. Both the light sheet thickness and the optical path will determine the measurement volume. As laser light sheets present thicknesses within the range of (or even exceeding) micron-sized flow cross sections, a microscope and microscope lenses are selected to illuminate and capture the flow field at microscale (Figure 7). On the other hand, in µPIV, the spacing between the microscope objective and the flow is limited. At the same time the optical access to the microfluidic flow can be limited to one direction only. Consequently, the

measurement plane is volume (or bulk) illuminated as the light is distributed through the microscope lens and captured through the same optical path.

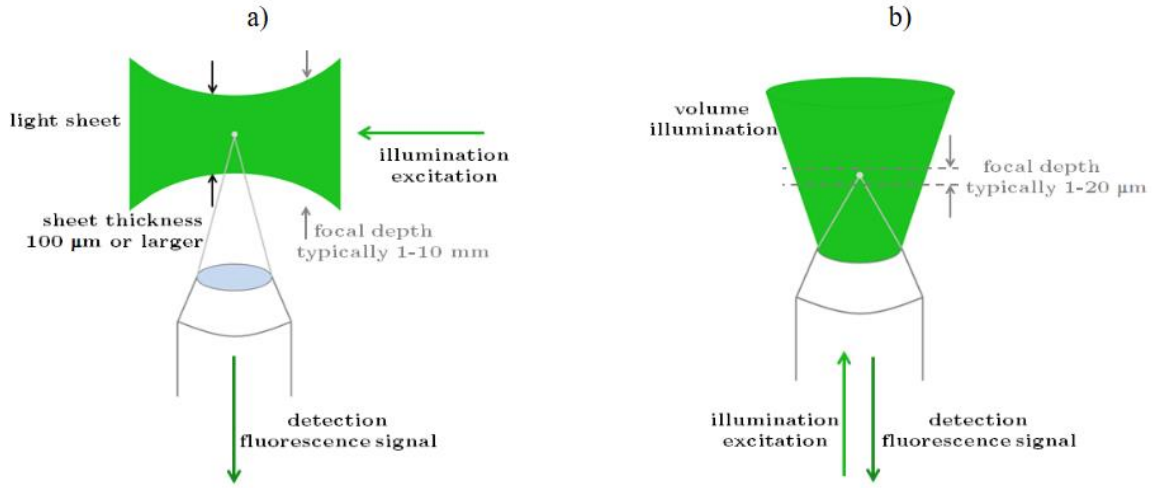

Figure 7: a) Orthogonal light sheet illumination and b) volume illumination in an inverted microscope [20].

4.3.2. Depth of field determination

For volume illumination, the measurement volume is defined by the magnification of the microscope objective. This magnification influences the measurement plane's thickness or depth of field δ_z, which is defined by the objective's magnification dependent numerical aperture (NA):

$$\delta_z = focal\ depth\ due\ to\ diffraction + focal\ depth\ due\ to\ geometrical\ effects$$

$$\delta_z = \frac{n\,\lambda_0}{(NA)^2} + \frac{n\,e}{(NA)\,M}$$

where n is the refractive index of the imaging medium, λ_0 is the wavelength of the imaged light in vacuum, e is the smallest distance resolved by the image detector placed in the microscope's image plane (on a CCD camera this would be the pixel-to-pixel spacing on the CCD chip) and M is the magnification of the objective. δ_z *is* a measure of the system's vertical resolution or a measure of twice the distance from the object plane in which the object is considered unfocused in terms of image quality.

In a µPIV system, the vertical resolution does not define the amount of information contained in the depth of field, as bright particles even if out-of-focus may contribute to the correlation function employed in the PIV analysis [21]. The quality of the information depends on the contrast between the bright fluorescent particles scattering light and the darker background. To collect information on the contribution of out-of-focus particles to the velocity measurement, the measurement depth is calculated. The measurement depth ($2 \cdot \delta_{z_m}$) is then defined as twice the distance from the object plane in which a particle becomes sufficiently unfocused that it no longer contributes significantly to

the velocity measurement. It includes the particle size as well as effects due to diffraction and geometrical optics.

$$\delta_{z_m} = \frac{3n\,\lambda_0}{(NA)^2} + \frac{2.16D_p}{tan\theta} + D_p$$

θ is the aperture angle of the objective lens and D_p is the diameter of the particle.

A detailed description of the various possible methodologies for the use of µPIV can be found in the literature [22], [23]. Usually, lasers are used to illuminate the flow. Pulsating lasers can be used quite conveniently to create thin and high intensity sheets of light [23]. Other light sources can be used as well [24], [25].

4.3.3. Tracer particle selection

As a final note on PIV, several aspects may influence the choice of particles for µPIV. A selection of three will be highlighted below [26]. For a more extensive explanation of particle selection see [27].

1. Individual particles need to be detected (fluorescence, backlight scatter) by the camera and be well resolved.
2. The particles need to have density similar to that of the fluid to guarantee they follow the flow (similar inertia and buoyancy) and do not influence it.
3. Particles need to have low enough inertia to follow rapid movement (high velocity, pulsatile flow, etc.)

5. Discussion

Looking at all the key performance parameters mentioned earlier, an efficient and reliable operation can be achieved if the flow of the microfluidic device is established as intended/designed. The following Figure 8 summarizes the influencing parameters for the flow and highlights negative aspects that may arise during operation. The methods to measure and characterize these parameters are partially mentioned in here and further guidelines will be established in this project to contribute to a better overview/understanding for the end-user.

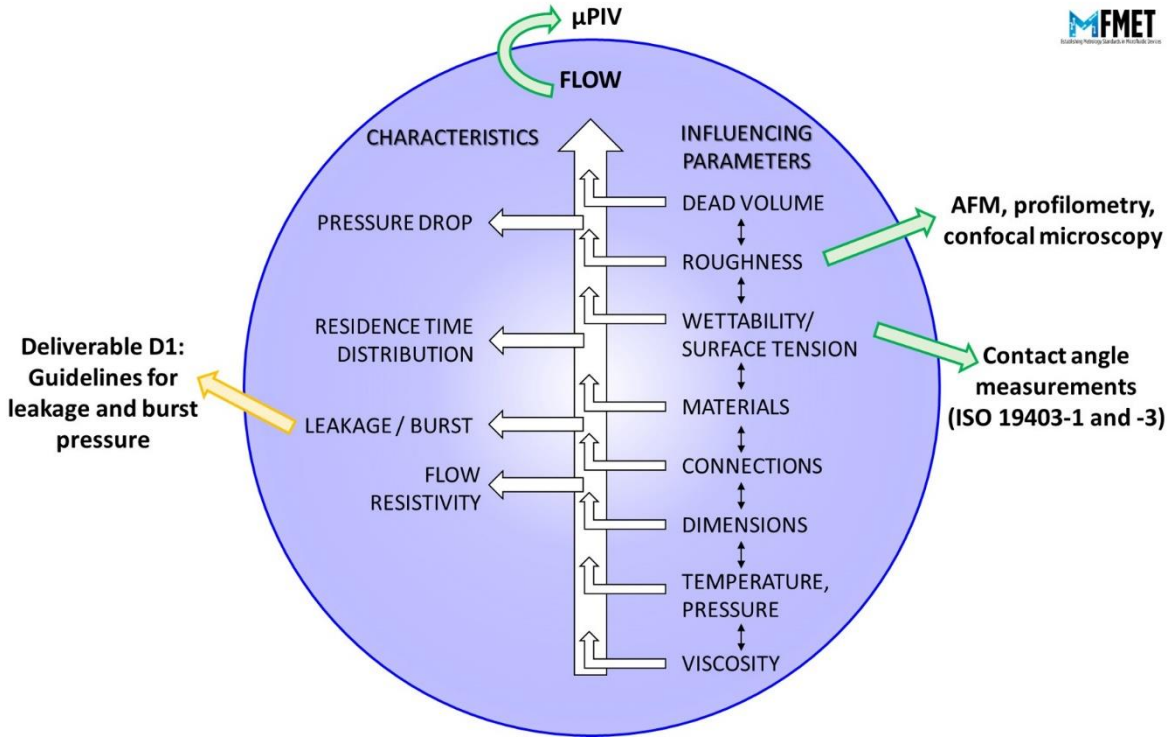

Figure 8: Overview of influencing parameters, characteristics and measurement methods concerning the flow in microfluidic devices.

It should be noted that it is not possible to distinguish clearly between the influencing parameters since each of them influences all the other parameters simultaneously.

For large channels, the flow rate is mainly governed by the pressure and the viscosity of the fluid, according to Laplace. For small channels, the interaction between the fluid and the channel wall begins to play a role. It is therefore necessary to accurately measure the material and fluid properties. Not only to understand and control the flow resistivity, but also fouling, biocompatibility etc. The measurement of these parameters mentioned here is only partly covered by existing ISO standards.

Materials

Since we only tested D263® bio samples, we would need the results from the polymer samples COC or COP, in order to have a comparison. In general, we can see that the contact angle is below 90°, therefore exhibiting a hydrophilic surface.

The same issue would apply for the characterization of the surface roughness of COC or COP samples, which is expected to be higher than for glass samples.

Wettability resp. surface energy

Using different liquids would provide a better regression line for the determination of the surface energy for a specific material (here: glass slides made of D263® bio).

Roughness

The glass wafer from the supplier exhibits a roughness specified below 0.5 nm. AFM measurements showed that the values for the roughness of both areas of interests (0.46 nm -0.60 nm) were in the range similar to the specified value (<0.5 nm) before the processing of the glass wafer. Interestingly, the surface roughness values for the channel are higher than for the bonding area. Therefore, it can be assumed that the wet etch process in glass does give a small increase to the initial surface roughness. It is also a good indication that the channels etched in glass do exhibit a very smooth surface, which is beneficial for the end application in microfluidics. Although only very small areas can be measured with AFM, the results are representative and give a good estimate of the roughness of all surfaces in a glass microfluidic.

The confocal microscope can be used to measure roughness, but this is dependent on the resolution of the instrument or method. The method can be used for coarse roughness values in the range of several µm, but this is not the case with these glass specimens. The method would be probably applicable on polymeric samples like COC or COP samples, since they can exhibit a roughness in the µm range.

In the stylus roughness measurements, no significant differences were found between the results of the measured roughness parameters *Ra*, *Rz*, *Rt*, *Rq*, *Rv* and *Rp*, neither inside the channels nor in the bonded areas. The results obtained for Rku with both techniques (confocal and stylus) are similar and close to the value of 3, although it is uncertain whether the value obtained with the confocal method is reliable due to the fact that it was measured below the resolution of the machine used.

Both measurement of macro-lines and micro-lines used for the roughness parameters determination are very important for the work in microfluidics as it allows a better understanding of the liquid surface path.

6. Conclusions and outlook

Key properties of microfluidic connectors are:

- Dead volume, i.e. the portion of the internal volume of a system that is not part of a continuous flow-path
- Ease of operation, including:
  → the time needed for mounting the connector, and for connecting/disconnecting it
  → the tooling required for mounting the connector, and for connecting/disconnecting it
- Pressure drop / Flow resistivity
- Leakage rate, i.e. the flow rate or flow rate range coming out of the fluidic path through the connector parts for a given pressure or pressure range respectively.
- Burst pressure, i.e. the pressure at which the sealing function, the continuity of the fluidic path and the integrity of the connectors parts assembly is not ensured.
- The number of times a connector can be reused.

Behind these properties are a several material / design related parameters:

- Dimensional: cross-section and length of the flow path
- Material properties: hydrophobicity, hydrophilicity, and wettability, roughness

Table 8: Overview of the parameters, its documentation, and corresponding issues.

Parameter	Standard or White Paper	Issues
Dead volume	ISO 7886-2	Measurement of dead volume is an unsolved problem in microfluidics.
Ease of operation		No guidelines for estimating this are available here.
Number of times a connector can be reused		No guidelines for estimating this are available.
Connections and dimensions	Guidelines with focus on connections and dimensions in progress (deliverable D6)	
Materials	White Paper on common microfluidic components materials: properties and fabrication available DOI: 10.5281/zenodo.7930231	
Pressure drop / Flow resistivity	Whitepaper flow resistivity available DOI 10.5281/zenodo.7919133. Development of test protocols for microfluidic devices available (A2.2.2) DOI 10.5281/zenodo.7845430. testing	
Leakage rate	White Paper protocols for leakage testing DOI: 10.5281/zenodo.6602162	No accurate and fast method for testing leakage of liquid of microfluidic devices
Burst pressure		
Dimensional (cross-section and length of the flow path)	ISO/CD 22916 - Microfluidic devices — Interoperability requirements for dimensions, connections and initial device classification	This is a general unsolved problem in microfluidics, especially in the case of polymer devices that are bonded
Pressure and temperature		
Hydrophobicity, hydrophilicity, and wettability	White Paper on the measurement of hydrophobicity, hydrophilicity, and wettability DOI: 10.5281/zenodo.7181091	
Roughness	ISO 4287 ISO 25178-2:2012 ISO 21920-3:2021 ISO 16610-21.	The choice of the method depends on the sample dimensions.
Residence Time Distribution		This was investigated by the earlier microfluidic ISO group, but never finalized
Viscosity	Test protocols for liquid properties related to microfluidic devices available (A2.3.2) DOI 10.5281/zenodo.7845224	

7. References

[1] http://www.microfluidicsinfo.com/wp-content/uploads/2017/08/DesignforManufacture-1.pdf

[2] ISO/FDIS 10991: 2023 Microfluidics — Vocabulary

[3] ISO 19403-1: 2017 Paints and varnishes — Wettability — Part 1: Terminology and general principles

[4] ISO 19403-2:2017 Paints and varnishes — Wettability — Part 2: Determination of the surface free energy of solid surfaces by measuring the contact angle

[5] Heshmati, M., & Piri, M. (2014). Experimental investigation of dynamic contact angle and capillary rise in tubes with circular and noncircular cross sections. *Langmuir*, *30*(47), 14151-14162

[6] Ehlers, S., Könemann, J., Ott, O., Wolf, H., Šetina, J., Furtado, A., & Sabuga, W. (2019). Selection and characterization of liquids for a low pressure interferometric liquid column manometer. *Measurement*, 132, 191-198

[7] A. Olanrewaju, M. Beaugrand, M. Yafia and D. Juncker, *Lab Chip*, 2018, **18**, 2323 **DOI:** 10.1039/C8LC00458G. Capillary microfluidics in microchannels: from microfluidic networks to capillaric circuits

[8] Son S, Chen L, Kang Q, Derome D, Carmeliet J. Contact Angle Effects on Pore and Corner Arc Menisci in Polygonal Capillary Tubes Studied with the Pseudopotential Multiphase Lattice Boltzmann Model. Computation. 2016; 4(1):12. https://doi.org/10.3390/computation4010012

[9] Valtteri Heiskanen, Kalle Marjanen, Pasi Kallio, Machine Vision Based Measurement of Dynamic Contact Angles in Microchannel Flows, Journal of Bionic Engineering, Volume 5, Issue 4, 2008, Pages 282-290, ISSN 1672-6529, https://doi.org/10.1016/S1672-6529(08)60172-9

[10] Jafari, Mohammad, and Jongwon Jung. 2017. "Direct Measurement of Static and Dynamic Contact Angles Using a Random Micromodel Considering Geological CO2 Sequestration" Sustainability 9, no. 12: 2352. https://doi.org/10.3390/su9122352

[11] ISO 25178-6:2010 Geometrical product specifications (GPS) — Surface texture: Areal — Part 6: Classification of methods for measuring surface texture

[12] ISO 25178-602:2010 Geometrical product specifications (GPS) — Surface texture: Areal — Part 602: Nominal characteristics of non-contact (confocal chromatic probe) instruments

[13] ISO 4287:1997 Geometrical Product Specifications (GPS) — Surface texture: Profile method — Terms, definitions and surface texture parameters (withdrawn; has been revised by ISO 21920-2:2021)

[14] ISO 12179:2021 Geometrical product specifications (GPS) — Surface texture: Profile method — Calibration of contact (stylus) instruments

[15] ISO 5436-1:2000 Geometrical Product Specifications (GPS) — Surface texture: Profile method; Measurement standards — Part 1: Material measures

[16] ISO 21920-3:2021 Geometrical product specifications (GPS) — Surface texture: Profile — Part 3: Specification operators

[17] ISO 3274:1996 Geometrical Product Specifications (GPS) — Surface texture: Profile method — Nominal characteristics of contact (stylus) instruments (reviewed and confirmed in 2017)

[18] Thielicke, W. (2014*). The Flapping Flight of Birds Analysis and Application*.

[19] http://www.dantecdynamics.com

[20] Silverio, V. (July 2016). *Micro-cooling technologies for high-density power systems*. Unpublished Ph.D. dissertation, Instituto Superior Técnico, Universidade de Lisboa, Lisboa, Portugal

[21] Meinhart C. D., Wereley S. T., Gray M. H. B. (2000). Volume illumination for two-dimensional particle image velocimetry, Measurement Science and Technology 11:809–814, doi:10.1088/0957-0233/11/6/326

[22] Doda, B. (2008). *Micro PIV*, https://velocimetry.net/micropiv_principles.htm

[23] Raffel, M., Willert, C. E., Wereley, S. T., & Kompenhans, J. (2007). *Particle Image Velocimetry: A Practical Guide*, 2nd Edition. Springer

[24] Hagsäter S.M., Westergaard C.H., Bruus H., Kutter J.P. (2008) Investigations on LED illumination for micro-PIV including a novel front-lit configuration. Exp. Fluids. 44:211–219. doi: 10.1007/s00348-007-0394-z

[25] Aguirre-Pablo A., Alarfaj M.K., Li E.Q., Hernández-Sánchez J.F., Thoroddsen S.T. (2017) Tomographic Particle Image Velocimetry using Smartphones and Colored Shadows. Sci. Rep. ;7:3714. doi: 10.1038/s41598-017-03722-9

[26] Kaal, J. (August 2021). Enabling Chip Characterization & Providing Chip Information, University of Twente., Enschede. The Netherlands

[27] Hasenberg, T. (2017). *Emulating the Human Vasculature in a Multi-Organ-Chip Platform Rheology and Vasculogenesis*